

Experimental response of RC columns built with plain bars under unidirectional cyclic loading



J. Melo & H. Varum

Dept. of Civil Engineering, University of Aveiro, Portugal

T. Rossetto

Dept. of Civil, Environmental & Geomatic Eng., University College of London, UK

A. Costa

Dept. of Civil Engineering, University of Aveiro, Portugal

SUMMARY:

A large number of existing reinforced concrete (RC) buildings structures were designed and built before mid-70's, when the reinforcing bars had plain surface and prior to the enforcement of the modern seismic-oriented design philosophies.

This paper describes a series of unidirectional cyclic tests performed on seven full-scale columns built with plain reinforcing bars, without adequate reinforcement detailing for seismic demands. The specimens have different reinforcing steel details and different cross sections. A further monotonic test was also carried out for one of the specimens and an additional column, built with deformed bars, was cyclically tested for comparison with the results for the specimens with plain bars. The main experimental results are presented and discussed. The influence of bond properties on the column behaviour is evidenced by differences observed between the cyclic response of similar specimens with plain and deformed bars. The influence of reinforcement amount and displacement history on the column response is also investigated.

Keywords: Plain reinforcing bars; Full-scale column tests; Cyclic behaviour

1. INTRODUCTION

The hysteretic behaviour of RC is highly dependent on the interaction between steel and concrete. Cyclic load reversals, such as the ones induced by the earthquakes, result in accelerated bond degradation and significant bar slippage. The bond-slip mechanism is reported to be one of the most common contributors to damage and collapse of existing RC structures subjected to earthquake loading (CEB 1996). This process can lead to failure at a cyclic stress level lower than the ultimate stress under monotonic loading (CEB 1996). Despite this, bond behaviour is usually disregarded in the analysis of RC structures and perfect bond between steel and concrete is frequently assumed.

The behaviour of RC elements built with plain reinforcing bars is particularly sensitive to the bond-slip mechanism. For instance, low bond capacities have a strong influence on fixed-end rotations, greatly increasing the bond-slip contribution to the element deformation, which may represent up to 80% to 90% of the element overall deformability (Melo *et al.* 2011; Verderame *et al.* 2008a,b, 2010). Experimental data about the cyclic behaviour of RC elements with substandard details built with plain reinforcing bars is scarce in comparison with available data for elements with deformed bars. Reports of recent experiments on columns, beams or beam-column joints with plain reinforcing bars can be found, for example in Verderame *et al.* 2008a,b, Prota *et al.* 2009, Fernandes *et al.* 2011a,b and on columns with deformed bars, for example Rodrigues *et al.* 2012. Also, existing literature on bond mechanisms of plain reinforcing bars is much less rich and detailed than that available for deformed bars, especially with regard to aspects of cyclic and post-elastic nature (Verderame *et al.* 2009).

In this paper the experimental results of the cyclic tests carried out on seven full-scale columns are presented. These columns are representative of typical columns in existing RC building structures built

without adequate reinforcement detailing for seismic loading, using plain reinforcing bars. A monotonic test was also performed on a specimen with the same details and properties as one of the specimens tested cyclically in order to compare the loading regimes. One additional column was built with deformed bars, to establish the performance comparison with the standard column built with plain bars. The influence of bond properties, lap-splice, reinforcement amount, cross-area section and cold joint, are also investigated.

2. EXPERIMENTAL CAMPAIGN AND MATERIAL PROPERTIES

2.1. Details of Column Specimens

The experimental campaign consisted in the unidirectional cyclic test of seven full-scale specimens, designed to represent columns with different cross sections and reinforcing steel details. In addition, an extra monotonic test was made to compare the results with the cyclic behaviour of another similar specimen. Each specimen represents a half-storey cantilever column in a building with three or four storeys. The specimen nomenclature adopted is: i) the first letter (C) refers to the columns specimens; ii) the second letter (P or D) refers to the reinforcing steel type, plain (P) or deformed (D); iii) the third letter (A to F) refers to the type of reinforcing details and amount, and the cross-section type.

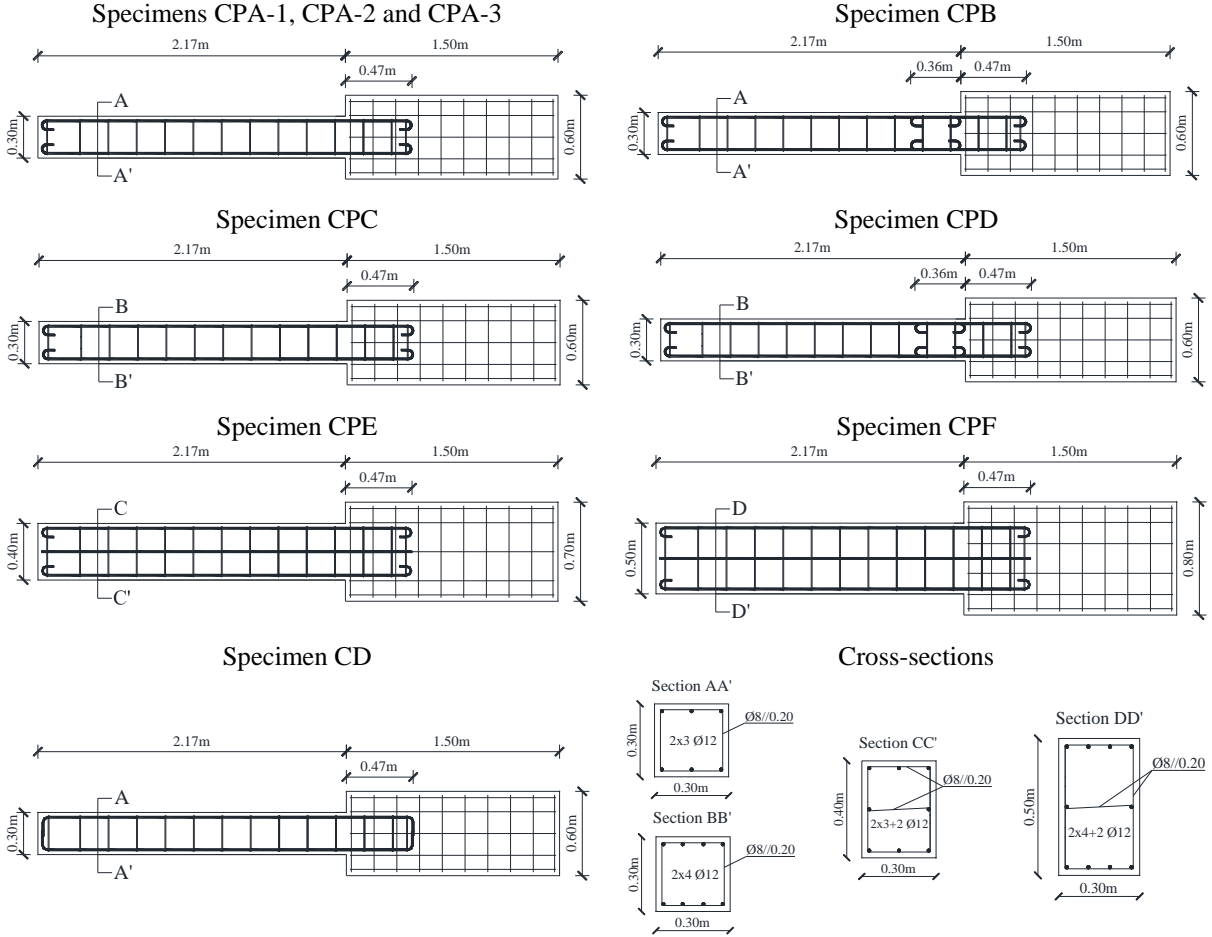


Figure 1. Geometry, dimensions and reinforcement detailing of specimens

Figure 1 shows the geometry, dimensions and reinforcement details of the specimens. Seven specimens (CPA-1,2,3, CPB, CPC, CPD and CD) had the same square cross-section with dimensions $0.30 \times 0.30 \text{ m}^2$. The other two specimens, CPE and CPF, had rectangular cross-section with dimensions $0.30 \times 0.40 \text{ m}^2$ and $0.30 \times 0.50 \text{ m}^2$, respectively. The length of column specimens is 2.17m, and the

foundations consist of a stiff RC block with a section of $0.30 \times (0.30 + \text{column cross-section width}) \text{m}^2$ and length equal 1.5m. The anchorage detailing of reinforcing plain bars were designed according to the first Portuguese codes RBA (1935) and REBA (1967) for reinforced concrete structures. The bar anchorage consist of end hooks. The lap-splice length adopted in specimens CPB and CPD were also designed according to the above mentioned Portuguese codes. The reinforcement ratio for longitudinal reinforcement (ρ_l) is equal to 0.75% and is the same in all specimens. The longitudinal reinforcing bar length inside the foundation is equal to 0.47m and corresponds to the normal length for a foundation with depth equal to 0.5m.

Specimen CPA-1 was cast in two phases: In the first phase the foundation was cast and in the second phase the column. This column simulated real construction phases, where the foundation and the column are cast at different times. Specimens CPA-2 and CPA-3 are identical to CPA-1 but were cast in a unique phase. Specimen CPB was similar to specimens CPA but included lap splicing of the reinforcing steel. Specimens CPC and CPD had larger amounts of reinforcing steel compared to the other specimens with square cross-section and the column CPD had a lap-splice. Specimens CPE and CPF had different reinforcing steel amount and different cross-sections compared to specimens CPA. Specimen CD was built with deformed bars and had the same reinforcing steel details and cross-section as specimens CPA.

Table 1 presents the mean values of the material properties of the concrete (cylinder samples - $\text{Ø}150\text{mm} \times 300\text{mm}$) and steel reinforcement used in each specimen. The specimens were cast using the same form work. All specimens were tested after 90 days of curing.

Table 1. Mean values of the material mechanical properties

| Specimen | Type of steel | Concrete | | Steel | | | | | |
|----------|---------------------|----------|-----------|----------|----------|----------|----------|----------|----------|
| | | (MPa) | | Ø 8 mm | | Ø 12 mm | | | |
| | | f_{cm} | f_{tcm} | f_{yk} | f_{uk} | E_{vm} | f_{yk} | f_{uk} | E_{vm} |
| CPA-1 | | 21.2 | 2.2 | | | | | | |
| CPA-2 | | 19.1 | 2.1 | | | | | | |
| CPA-3 | | 17.4 | 2.1 | | | | | | |
| CPB | A235 - Plain | 20.3 | 2.2 | 410 | 495 | 198 | 405 | 470 | 199 |
| CPC | | 17.1 | 2.1 | | | | | | |
| CPD | | 18.0 | 1.9 | | | | | | |
| CPE | | 18.0 | 1.9 | | | | | | |
| CPF | | 18.3 | 2.0 | | | | | | |
| CD | A400NRSD - Deformed | 17.1 | 2.0 | 470 | 605 | 198 | 465 | 585 | 199 |

2.2. Loading Conditions and Test Setup

Figure 2 shows the test setup adopted, the imposed loading and the lateral displacements imposed at the top of the columns. The specimens were tested in the horizontal position in a new test setup. Two devices with high load-carrying capacity and reduced friction were placed below the column and two concrete blocks were placed below the foundation to carry the elements' self-weight.

The cyclic tests were carried out under displacement-controlled conditions. Two hydraulic actuators were arranged at the top of the columns: one to impose the lateral displacements (d_c) and another for the axial force (N). The cyclic lateral displacement history adopted is presented in Figure 2-a. Three cycles were applied for each of the following peak drift values (\pm %): 0.1, 0.2, 0.3 and than 0.5 to 5.5 with 0.5 increments. Several tests were stopped before 6.5% drift. In specimen CPA-2, an increasing displacement load was applied monotonically in the negative direction up to 9% drift. The axial force was constant and equal to 305kN in all tests.

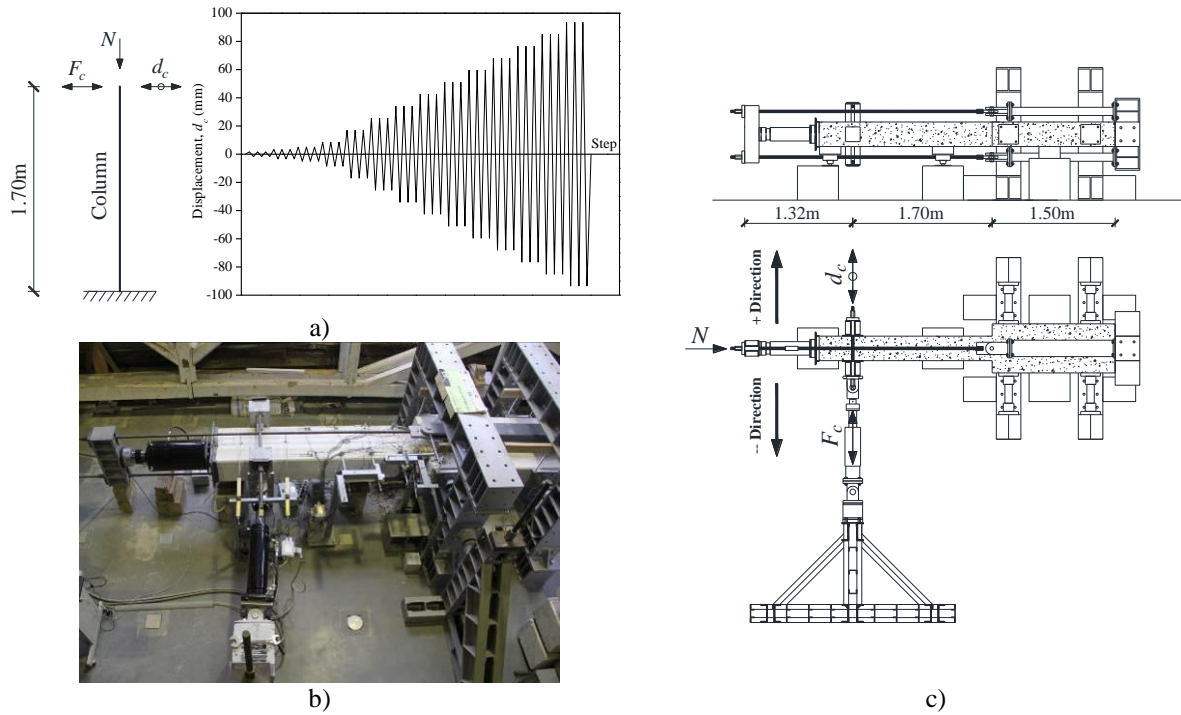


Figure 2. Test apparatus: a) support and loading conditions idealized and lateral displacement history imposed; b) general view; c) test setup schematics

3. EXPERIMENTAL RESULTS

In this section, the main results from the experimental campaign are presented. Firstly, the envelopes of the force-displacement diagrams are shown. Secondly, the evolution of the hysteretic dissipated energy with the drift level is presented. Finally, the equivalent damping-displacement ductility relationships are provided. Several comparisons are established between the cyclic results, in terms of force-displacement relationships to show the impact of the amount or detailing of reinforcing steel and cross-sections dimensions on the cyclic behaviour. The cyclic response of two specimens built with plain and deformed bars are compared. Finally, the damage state is shown and discussed. It should be noted that the results of specimen CD are presented only up to the drift value of 3.5% and not 5% due to problems with data acquisition system. However, the damage state shown corresponds to 5% of drift.

3.1. Global Results

Figure 3 compares the force-displacement envelopes, evolution of the dissipated energy and the equivalent damping-displacement ductility diagrams obtained from the experimental results. The hysteretic dissipated energy was computed for all cyclic tests performed as the sum of the area under the force-displacement diagrams. For each drift amplitude level, the plotted value of dissipated energy corresponds to the end of the third cycle. In the hysteretic dissipated energy diagrams the large mark corresponds to the ultimate point. The equivalent damping (ζ_{eq}) was computed according to Varum (2003) and Priestley *et al.* (2007). The displacement ductility (μ_d) corresponds to the ratio between the imposed displacement (d_c) and the yielding displacement (Δy , Table 2).

In Table 2 the values of maximum applied force ($F_{c,max}$) and the corresponding drift ($Drift_{F_{c,max}}$) are presented together with the ultimate force ($F_{c,ult}$) and corresponding drift ($Drift_{F_{c,ult}}$). The yielding force and yield displacement are also presented in Table 2, which were computed according to Annex B.3 of Eurocode 8 (elasto-perfectly plastic force-displacement relationship). The fitting of the elasto-perfectly plastic relationship was made to the ultimate point of the force-displacement envelopes. The ultimate force corresponds to the conventional element failure, i.e. when the strength has a reduction

of 20% relatively to the maximum force, as adopted by Park and Ang (1987). For specimen CPA-2 (monotonic test), the maximum strength reduction was 7.5% for 9.0% of drift, consequently the conventional ultimate point was not achieved.

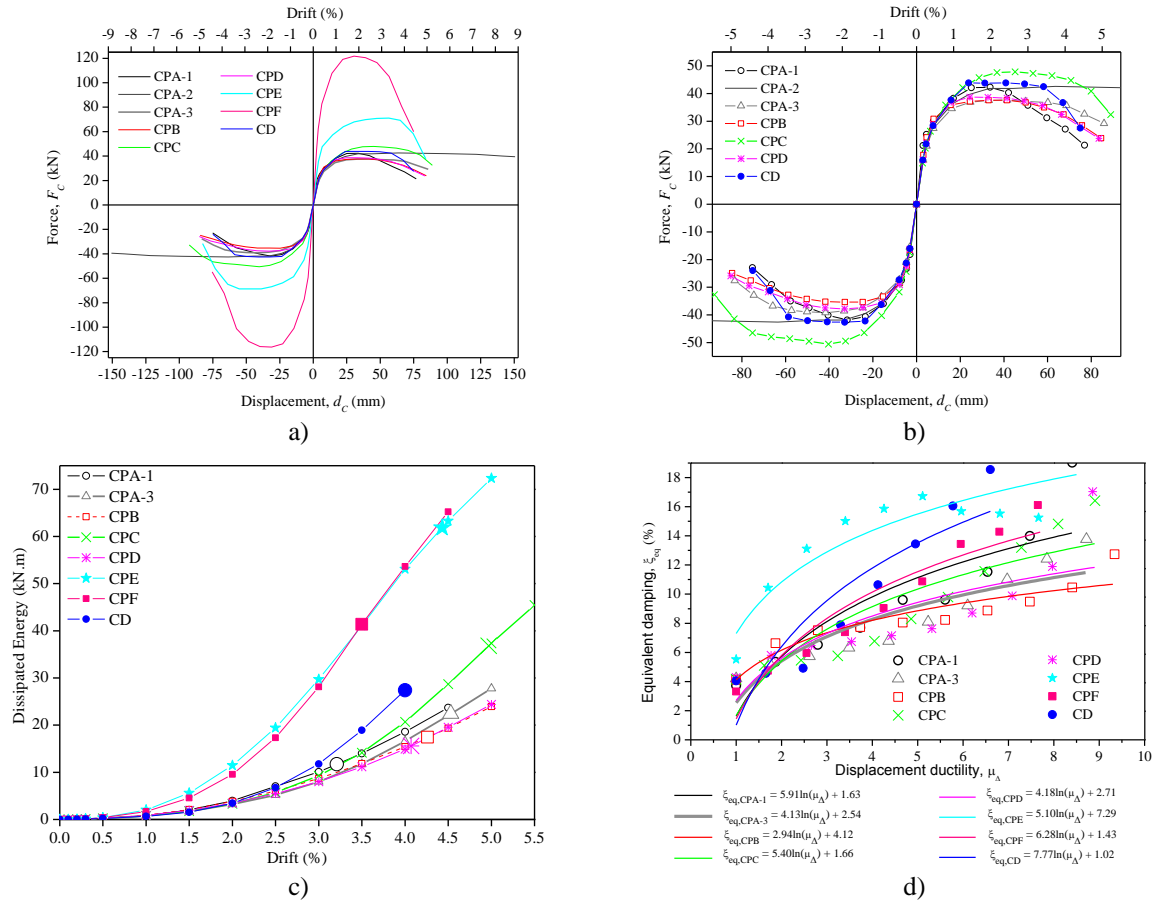


Figure 3. Global results: a) and b) force-displacement envelopes; c) hysteretic dissipated energy evolution; d) equivalent damping-displacement ductility diagram

Table 2. Maximum and ultimate force, drift values and yielding displacement

| Specimen | Max. force, $F_{c,max}$ (kN) | Drift $_{F_c,max}$ (%) | Ult. force, $F_{c,ult}$ (kN) | Drift $_{F_c,ult}$ (%) | Yielding force (kN) | Δ_y (mm) |
|----------|---------------------------------|---------------------------|---------------------------------|---------------------------|------------------------|-----------------|
| CPA-1 | 42.3 | 1.98 | 33.8 | 3.21 | 38.7 | 9.10 |
| CPA-2 | 42.6 | 3.73 | - | - | 40.9 | 10.10 |
| CPA-3 | 39.2 | 2.45 | 31.3 | 4.53 | 36.2 | 9.75 |
| CPB | 37.6 | 2.43 | 30.1 | 4.26 | 34.9 | 9.10 |
| CPC | 50.6 | 2.37 | 40.4 | 4.97 | 45.4 | 10.50 |
| CPD | 38.7 | 1.43 | 30.9 | 4.07 | 36.2 | 9.60 |
| CPE | 71.1 | 3.32 | 56.9 | 4.43 | 65.6 | 9.98 |
| CPF | 121.7 | 1.79 | 97.4 | 3.50 | 112.3 | 10.00 |
| CD | 43.8 | 1.40 | 35.1 | 4.00 | 40.7 | 10.30 |

The variation in maximum force of the specimens with square cross-section and same amount of reinforcing steel was 5.0kN, i.e. 12% of the maximum strength. In specimen CPA-1, that was a cold joint between the column and foundation interface, the maximum strength was achieved for a lower drift value (1.98%) than in specimen CPA-3 (2.45%), and the same conclusion can be draw for the ultimate point. As a consequence, the specimen with cold joint shows a larger strength degradation and a 48% lower dissipated energy until ultimate point than the standard specimen (CPA-3). The specimen CPA-2, tested monotonically, shows similar initial stiffness but a maximum strength that is 8% greater than specimen CPA-3. The amount of strength degradation is also observed to be very

small, compared to the cyclic tests.

Specimen CPB displays a larger initial stiffness, similar maximum strength, greater strength degradation and 22% less dissipated energy (considering the ultimate point) than specimen CPA-3. Specimen CPC shows a similar initial stiffness, larger peak force (29% more) and 64% greater dissipated energy until the ultimate point than specimen JPA-3. Specimen CPD displays a similar initial stiffness, lower peak force (24% less) and 57% less dissipated energy until the ultimate point than specimen CPC. Specimen CD exhibits a similar initial stiffness, larger peak force (12% more) and 22% greater dissipated energy (until ultimate point) than specimen CPA-3.

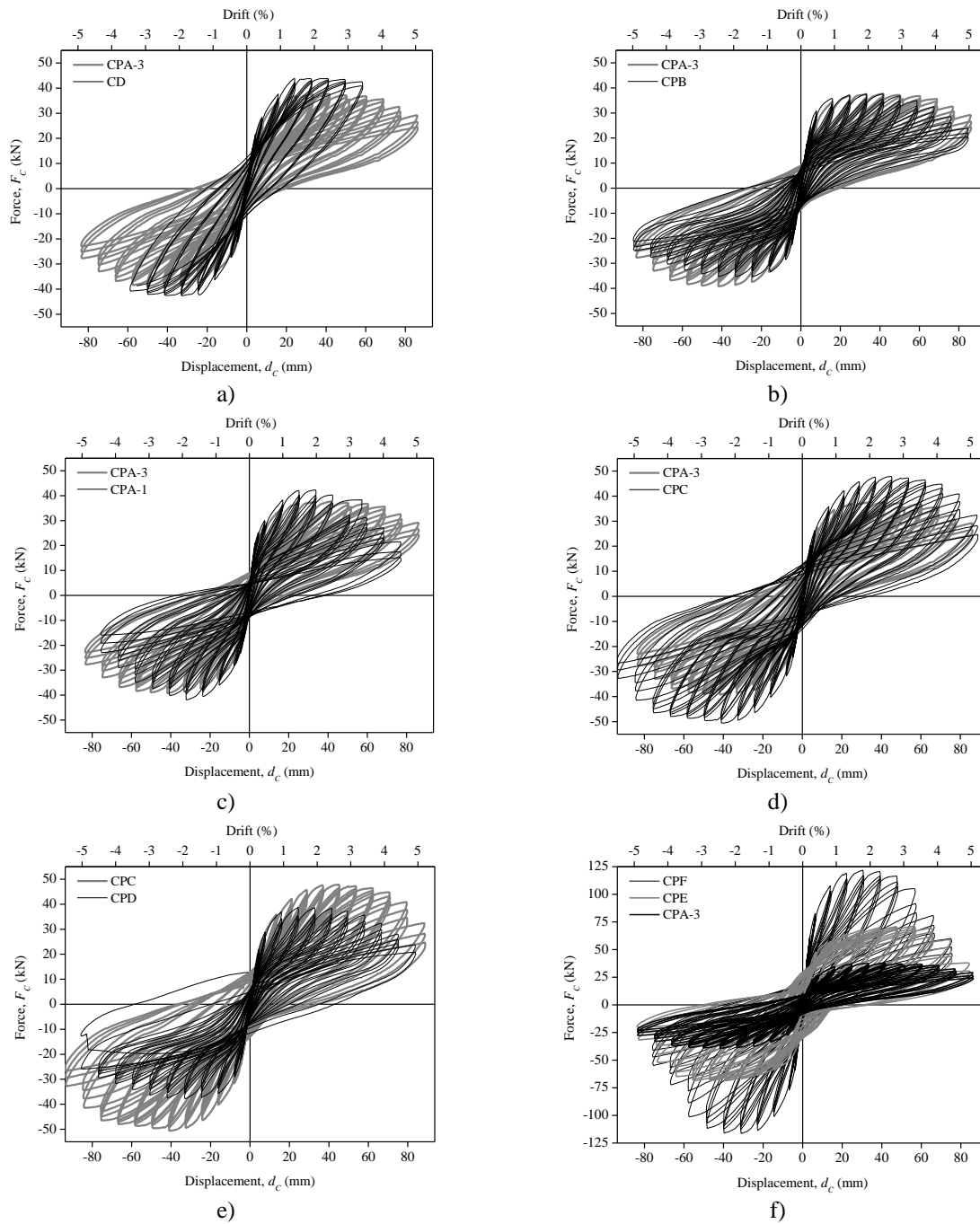


Figure 4. Force-displacement diagram comparison

When the column section depth increases (specimens CPE and CPF), both the initial stiffness and the peak force increase. Despite the fact that the peak force in specimen CPF is 71% higher than in

specimen CPE, specimen CPE presents a larger dissipated energy (+49%) than specimen CPF. Pinching is seen to influence the dissipated energy and explains the lower dissipated energy in specimen CPF.

The best fit curves of the equivalent damping-displacement ductility relationships determined from the experimental results are shown in Figure 3-d. For displacement ductility $\mu_{\Delta} \geq 2.0$, the specimen with deformed bars (CD) presents larger equivalent damping than other specimens with the same cross-section dimensions. It also has the largest in equivalent damping with displacement ductility. It shows that the better bond conditions provided by deformed bars increase the equivalent damping. Specimens CPC and CPD with higher amounts of steel, show higher equivalent damping than the standard specimen. Specimens with lap-splice present lower equivalent damping than the specimens with continuous longitudinal reinforcing steel for displacement ductility $\mu_{\Delta} > 3.0$. For a displacement ductility of 1, the equivalent damping has a variation between 1% and 4% in the square columns. These values are lower than the 5% indicated in Priestley *et al.* (2007) for concrete frame buildings.

Figure 4 shows the lateral force-drift diagrams for all specimens and in the same diagram are plotted more than one curve. Specimen CD shows larger unloading and reloading stiffness than specimen CPA-3. The pinching effect in specimen CPB is more evident than in specimen CPA-3 and also in specimen CPA-1 the same conclusion can be drawn. In specimen CPC the pinching effect is similar to that in specimen CPA-3 and less marked than in specimen CPD. The pinching effect is analogous in specimens CPA-3 and CPF, but is less evident in specimen CPE.

3.2. Damage observed

Figure 5 illustrates the crack pattern observed at the end of the test for all columns. Specimens with lap-splice display concrete spalling along the lap-splice length.

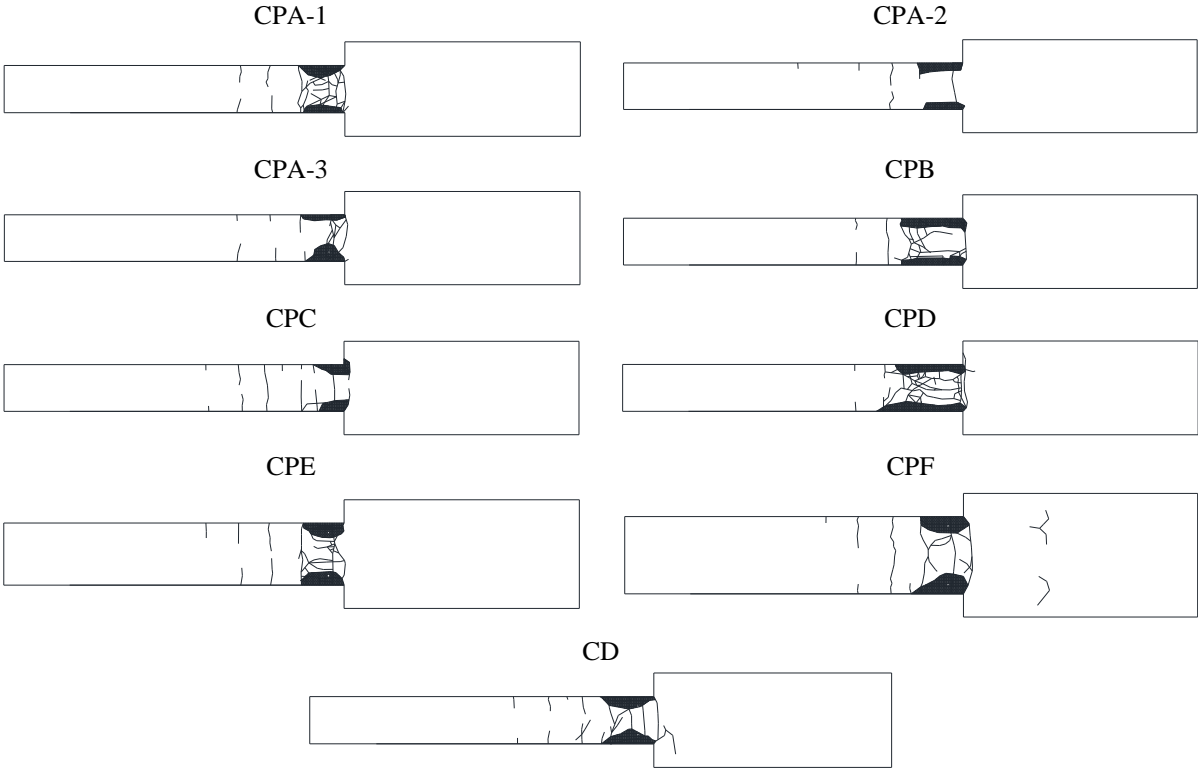


Figure 5. Damage state at the end of the tests

The specimens without lap-splice show concrete spalling approximately along 0.27m measured from the base of the column and in the specimens with larger depth (CPE and CPF) the concrete spalling is

not limited to the cover but includes part of the core. Specimen CPA-1 show more cracks in the plastic hinge region than specimen CPA-3 because the cold joint in specimen CPA-1 causes concrete discontinuity, weakening the concrete in the plastic hinge zone. Specimen CPD had high damage in the concrete at the plastic hinge due to stress concentrations caused by the presence of the anchorage hooks. Comparing the final damage in specimens CPB and CPD with the same reinforcing details but with different amounts of steel, column CPD shows more longitudinal cracks in the plastic hinge region because the concrete fails in compression between the hooks of the longitudinal bars in the lap-splice. In specimen CPA-3 the damage was more concentrated in the column-foundation interface, while in column CD the damage was distributed along a length equal to the cross-section depth at the column base.

4. FINAL COMMENTS

Experimental tests were carried out to assess the cyclic and monotonic behaviour of full-scale columns with plain bars and poor reinforcement detailing. The influence of bond properties, lap-splice, reinforcement amount, cross-area section and cold joint, on the cyclic behaviour of the columns was investigated. Tests results were analyzed in terms of initial stiffness, maximum strength, strength degradation, hysteretic dissipated energy, equivalent damping function of displacement ductility and damage state at the end of the tests. From the analysis of the experimental results, the following main conclusions can be drawn:

- The influence of the cold joint between column and foundation on the cyclic behaviour is: i) a larger strength degradation; ii) an increase in the concrete damage at the plastic hinge; and iii) a considerable drop in the dissipated energy;
- The lap-splice affects the cyclic behaviour of the columns, decreasing the dissipated energy of the specimens and increasing the damage in the plastic hinge zone;
- The lap-splice decreases the equivalent damping for lower values of displacement ductility and increases the pinching effect;
- When the amount of steel is higher and there are lap-splices, the concrete fails in compression due to the large stresses provided by the bar hooks. In this case, the maximum strength of the column is not achieved;
- The strength degradation in the monotonic test was small and the ultimate point was not achieved until 9% of drift. However, in Verderame *et al.* (2008a) the strength degradation was more evident for similar column tests, and the ultimate point was achieved in some specimens at 6% of drift. In the monotonic tests performed by Verderame *et al.* (2008a), the drift value corresponding to the maximum force is approximately half of the drift value corresponding to the maximum force achieved in specimen CPA-2;
- The drift values corresponding to the maximum strength in the columns without and with lap-splice are approximately 85% and 40% higher than the drift values in similar tests carried out by Verderame *et al.* (2008b), respectively;
- Columns built with plain bars dissipated less energy and the equivalent damping values are lower than the column built with deformed bars;
- The cracks on the specimen built with deformed bars are more spread along the span compared to the specimens built with plain bars. This is an agreement with observations made by Fernandes *et al.* (2011c) in their tests;
- Columns with large cross-section can dissipate less energy than other with smaller cross-section, due to the pinching effect.

The differences observed between the response of the columns CPA-3 and CD, demonstrates the significant influence of the bond properties in the cyclic response of RC columns. The slippage between reinforcing bars and the surrounding concrete should be considered in the seismic performance assessment of existing RC building structures.

ACKNOWLEDGEMENT

The authors acknowledge the staff of the Civil Engineering Laboratory at the University of Aveiro for the support in the preparation and implementation of the testing setup and campaign. This paper reports research developed under financial support provided by “FCT - Fundação para a Ciência e Tecnologia”, Portugal, namely through the PhD grant of the first author, with reference SFRH/BD/62110/2009.

REFERENCES

- CEB (1996). RC Elements under Cyclic Loading. State of-the-art report, Thomas Telford Ltd., London, UK.
- CEN (2004). EN 1998-1:2004. Eurocode 8: Design of structures for earthquake resistance – 19 Part 1: General rules, seismic actions and rules for buildings, European Committee for 20 Standardization, Brussels.
- Fernandes, C., Melo, J., Varum, H. and Costa, A. (2011a). Cyclic behavior of a two-span RC beam built with plain reinforcing bars, *Periodica Polytechnica Civil Engineering* **55:1**, 21-29.
- Fernandes, C., Melo, J., Varum, H. and Costa, A. (2011b). Cyclic behavior of substandard RC beam-column joints with plain bars, *ACI Structural Journal*, (accepted for publication).
- Fernandes, C., Melo, J., Varum, H. and Costa, A. (2011c). Comparative analysis of the cyclic behavior of beam-column joints with plain and deformed reinforcing bars, *IBRACON Structures and Materials Journal* **4:1**,147-172.
- Governo, D. (1935). Regulamento do Betão Armado (RBA), Decreto n.º 25948, 16 de Outubro, serie I, num. 240, Lisbon.
- Governo, D. (1967). Regulamento de Estruturas de Betão Armado (REBA), Decreto n.º 47723, 20 May, serie I, num. 119, Lisbon.
- Rodrigues, H., Varum, H., Arêde, A. and Costa, A. (2012). A comparative analysis of energy dissipation and equivalent viscous damping of RC columns subjected to uniaxial and biaxial loading. *Engineering Structures, Elsevier* **35**,149-164.
- Melo, J., Fernandes, C., Varum, H., Rodrigues, H., Costa, A. and Arêde, A. (2011). Numerical modelling of the cyclic behaviour of RC elements built with plain reinforcing bars. *Engineering Structures, Elsevier* **33:2**,273-286.
- Park, Y. J., Ang, A. H. S., and Wen, Y. K., (1987). Damage-limiting aseismic design of buildings, *Earthquake Spectra* **3:1**,1-26.
- Priestley, M., Calvi, G. and Kowalsky, M. (2007). Displacement-Based Seismic Design of Structures, IUSS PRESS, Italy.
- Prota, A., Cicco, F. and Cosenza, E. (2009). Cyclic Behavior of Smooth Steel Reinforcing Bars: Experimental Analysis and Modeling Issues, *Journal of Earthquake Engineering* **13:4**,500-519.
- Varum, H. (2003). Seismic assessment, strengthening and repair of existing buildings, PhD Thesis, University of Aveiro, Portugal.
- Verderame, G.M., Fabbrocino, G. and Manfredi, G. (2008a). Seismic Response of R.C. Columns with Smooth Reinforcement. Part I: Monotonic Tests, *Engineering Structures* **30:9**,2277-2288.
- Verderame, G.M., Fabbrocino, G. and Manfredi, G. (2008b). Seismic Response of R.C. Columns with Smooth Reinforcement. Part II: Cyclic Tests, *Engineering Structures* **30:9**,2289-2300.
- Verderame, G.M., Ricci, P., Carlo, G.D. and Manfredi G. (2009). Cyclic Bond Behavior of Plain Bars. Part I: Experimental Investigation, *Construction and Building Materials* **23:12**,3499-3511.
- Verderame, G.M., Ricci, P., Manfredi, G. and Cosenza E. (2010). Ultimate Chord Rotation of RC Columns with Smooth Bars: Some Considerations about EC8 Prescriptions, *Bulletin of Earthquake Engineering*, **8:6**,1351-1373.